Li–S Battery

DOI: 10.1002/anie.201100637

Porous Hollow Carbon@Sulfur Composites for High-Power Lithium–Sulfur Batteries**

*N. Jayaprakash, J. Shen, Surya S. Moganty, A. Corona, and Lynden A. Archer**

Among cathode materials for secondary lithium batteries, elemental sulfur has the highest theoretical capacity, 1672 $mA\,h\,g^{-1}$ against lithium, which is at least ten times greater than that of commercially used transition-metal phosphates and oxides. As a cathode, sulfur hosts two lithium ions non-topotactically, supporting the electrochemical redox reaction $16\,Li + S_8 \rightleftarrows 8\,Li_2S$.[1] Other advantages of using sulfur as the cathode material for batteries are its low cost and widespread availability; its intrinsic protection mechanism from overcharging, which enhances battery safety; a wide operating temperature range; and the potential for a long life cycle.[2,3] Sulfur has consequently been studied extensively as a cathode material and is considered a promising candidate for electric and hybrid electric vehicles.[4]

Despite this promise, implementation of Li–S secondary battery systems for high power applications has been problematic. Hindered by the inherent poor electrical conductivity of sulfur (5×10^{-30} $S\,cm^{-1}$ at 25 °C) and shuttling of higher-order polysulfides during charging, a commercially viable Li–S cell is yet to be realized.[4] Sulfur's low electrical conductivity limits active material utilization as a result of poor electrochemical contacts within the material. Shuttling is a cyclic process in which long-chain lithium polysulfides, (Li_2S_n, $2 < n < 8$), generated at the cathode during charging, dissolve into the electrolyte and migrate to the anode where they react with the lithium electrode in a parasitic fashion to generate lower-order polysulfides, which diffuse back to the sulfur cathode and regenerate the higher forms of polysulfide.[5] This shuttling process is driven by the concentration gradient of polysulfide and there are literature reports which suggest that it provides a potential benefit for overcharge protection in Li–S batteries.[6] However, left unchecked, it leads to decreased utilization of the overall active material mass during discharge, triggers current leakage, poor cycleabilty, and reduced columbic efficiency of the battery.[7]

Over the last three decades, methods for preventing polysulfide dissolution and shuttling in Li–S secondary batteries have been intensively investigated by research teams world-wide. One line of study focuses on tailoring the electrolyte to restrain polysulfide dissolution. Electrolytes based on THF, THF/toluene and dioxolane, for example, have been reported to facilitate utilization of sulfur at low discharge currents (0.01 $mA\,cm^{-2}$),[8] which corresponds to a two-month discharge. An electrolyte formulation based on lithium triflate in tetraglyme has been reported to be effective in controlling shuttling in Li–S batteries, but with an unacceptably low efficiency of 48 %.[9] Room temperature ionic liquids have recently attracted attention as electrolytes for Li–S batteries due to their nonflammability, nonvolatility, wide electrochemical window, and thermal and chemical stabilities.[10] Unfortunately, high interfacial impedance at the Li metal electrode limits the rate capability and long-term cycle life of the Li–S batteries.[11] Persistent efforts to safeguard the lithium anode[12] and to reduce mobility of the polysulfide anions in the electrolyte[13] have also proven largely ineffective in enhancing the cycle life and capacity fading in Li–S batteries.[14]

An alternative method utilizes composite sulfur powder coated with conducting polymers to prevent shuttling. This approach has attracted significant interest as certain properties of conducting polymers, including their morphology and electrochemical stability, have been shown to produce stable composites, which yield capacities ranging from 500 and 800 $mA\,h^{-1}$ after 50 cycles at low (100 $mA\,g^{-1}$) current rates.[15] Even under these conditions, however, lithium polysulfide dissolution persists and other cathode configurations including organic sulfides like DMcT (2,5-dimercapto-1,3,4-thiadiazole), electropolymerized conductive polyaniline, CuS, and FeS_2 have been actively studied with some success.[16] The specific capacity (280 $mA\,h\,g^{-1}$) of the most promising of these compounds is nonetheless significantly lower than that of elemental sulfur. Metal oxide adsorbents such as silicates, aluminum oxide, vanadium oxide, and metal chalcogenides have been proposed as inhibitors for polysulfide dissolution, but only with limited success.[17] Carbonaceous sorbents with controlled morphology and structural stability have been more successful,[18] with the most notable example coming from the elegant, recent work of Nazar et al.,[1] which utilize highly ordered, mesoporous carbon capable of sequestering sulfur and polysulfides. At a low discharge rate of 168 $mA\,g^{-1}$ (0.1 C), these authors reported that capacities in excess of 800 $mA\,h\,g^{-1}$ can be maintained in the pristine carbon material for 20 cycles, with some fading. Addition of a thin polymer coating on the carbon leads to improved electrochemical behavior, but extended cycle life and rate capability data were not reported.

Here we report a facile, scalable approach for synthesizing mesoporous hollow carbon capsules that encapsulate and sequester elemental sulfur in its interior and porous shell. The

[*] N. Jayaprakash, J. Shen, S. S. Moganty, A. Corona, Prof. L. A. Archer
School of Chemical and Biomolecular Engineering
Cornell University, Ithaca, NY 14853-5201 (USA)
E-mail: laa25@cornell.edu

[**] This material is based on work supported as part of the Energy Materials Center at Cornell, an Energy Frontier Research Center funded by the U.S. Department of Energy, Office of Basic Energy Sciences under Award Number DE-SC0001086.

Supporting information for this article is available on the WWW under http://dx.doi.org/10.1002/anie.201100637.

interior void space, mesoporous shell structure, chemical make-up of the shell, and the methodology used to infuse sulfur into the capsules are designed with four specific aims in mind: 1) maximize the amount of sulfur sequestered by the capsules; 2) minimize lithium polysulfide dissolution and shuttling in the electrolyte; 3) preserve fast transport of lithium ions to the sequestered sulfur by ensuring good electrolyte penetration; and 4) facilitate good transport of electrons from the poorly conducting sulfur. Used as the cathode material in Li–S secondary batteries, the as prepared C@S carbon–sulfur nanocomposite capsules are found to manifest promising electrochemical behavior upon extended cycling for 100 cycles at 850 mA g^{-1} (0.5 C), consistent with our goals in designing the capsules. The electrochemical stability of the C@S composites is confirmed using extended scan cyclic voltammetry measurements.

In the first step of the synthesis, carbon spheres are created by pyrolysis of a low-cost carbon precursor (pitch) uniformly deposited onto and into porous metal oxide nanoparticles (Supporting Information, Figure S1a,b). Subsequent dissolution of the nanoparticle support yields well-defined hollow, mesoporous carbon spheres (Figure 1a). By

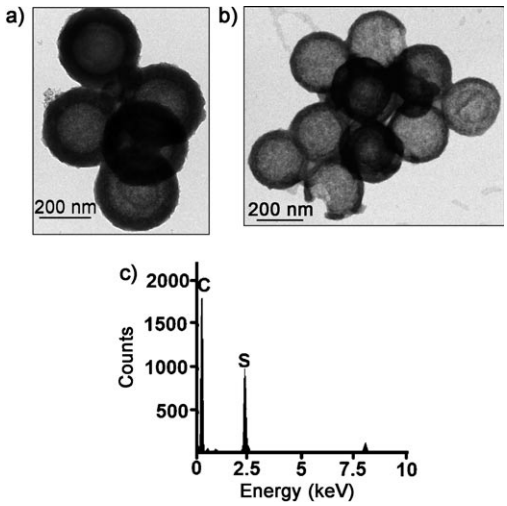

Figure 1. TEM images of a) mesoporous carbon hollow spheres b) C@S nanocomposite and c) EDX analysis of C@S nanocomposite showing the presence of sulfur.

manipulating the metal oxide particle size and porosity, hollow carbon spheres with high specific surface area of 648 $m^2 g^{-1}$, 3 nm average pore diameter (Figure S2a,b), and large internal void space (Figure 1a) were facilely created. In the final step of the synthesis, we take advantage of the relatively low sublimation temperature of sulfur to infuse gaseous sulfur into the carbon support present in one compartment of a dual-compartment segmented tube.[19] This methodology facilitates fast, efficient, and controlled infusion of elemental sulfur into the host carbon porous structure and yields particles with tap density of around 0.82 g cm^{-3}. Thermal gravimetric analysis (Figure S3) shows that approximately 35% sulfur can be incorporated in the particles in a single pass, and that by three passes (i.e. repeat exposures of the porous carbon particles to sulfur vapor), nearly 70% of the mass of the porous particles is comprised of sulfur.

Figure 1a,b shows the TEM images of typical carbon hollow spheres before and after sulfur infusion. The high surface area and relatively large mesopore sizes are attractive because they should allow the electrolyte and Li ions produced from the Li–S redox reaction to penetrate the structure. While creating occasional ruptures in the walls of the hollow carbon spheres (e.g. see leftmost sphere in Figure 1b), the pressure built-up in the pyrex tube is considered essential for facilitating complete incorporation of sulfur into the carbon host.[19] Elemental composition of the C@S nanocomposites analyzed by energy-dispersive X-ray (EDX) microanalysis is shown in Figure 1c. EDX spectra collected from different locations within the mesoporous C@S material also indicate the presence of sulfur throughout the carbon hollow spheres.

Elemental sulfur generally exists in a very stable orthorhombic crystalline structure. The absence of characteristic peaks for crystalline sulfur in the X-ray diffraction pattern (Figure S4) indicates a very low degree of crystallization in C@S nanocomposite. This suggests that the sublimed sulfur is amorphous or that the sulfur particles trapped in the mesoporous carbon spheres are unable to crystallize. XRD indicates, however, that the carbon material has some crystalline order, which is indicative of graphitic character for the materials studied here. The relative peak areas can be analyzed to estimate the degree of graphitization or the orientation of graphite planes. This analysis (Figure S5) indicates that more than 38% of the material is graphitic carbon. The relative intensity of the D- and G-Raman scattering peaks at 1350 and 1580 cm^{-1}, respectively, provides a well-known alternative method for identifying carbon, as well as for assessing its graphitic content.[20] The presence of both the D- and G-Raman bands in the carbon spheres is confirmed in the spectrum shown in Figure S6. The graphitic content can be estimated to be around 16%; we attribute the difference between the two estimates to the lower quality of the Raman calibration curve (Figure S7). Because the electrical conductivity of graphitic carbon is substantially higher than of amorphous carbon, even partially graphitized carbon nanospheres are attractive because they facilitate transport of electrons from the poorly conducting sulfur, aiding electrochemical stability of the C@S nanocomposite capsules even at high dicharge rates.

A cyclic voltammogram (CV) of the C@S nanocomposite is shown in Figure 2a. The pair of sharp redox peaks indicates that during charge/discharge the electrochemical reduction and oxidation of sulfur occurs in two stages. The first peak at 2.4 V involves the reduction of elemental sulfur to lithium polysulfide (Li_2S_n, $4 \le n < 8$). The second peak at 2.0 V involves the reduction of sulfur in lithium polysulfide to Li_2S_2 and eventually to Li_2S. The oxidation process in the Li–S cell also occurs in two stages. The oxidation peak at 2.35 V is associated with the formation of Li_2S_n ($n > 2$). This process continues until lithium polysulfide is completely consumed and elemental sulfur produced at 2.45 V.[2] Significantly, no changes in the CV peak positions or peak current (inset in

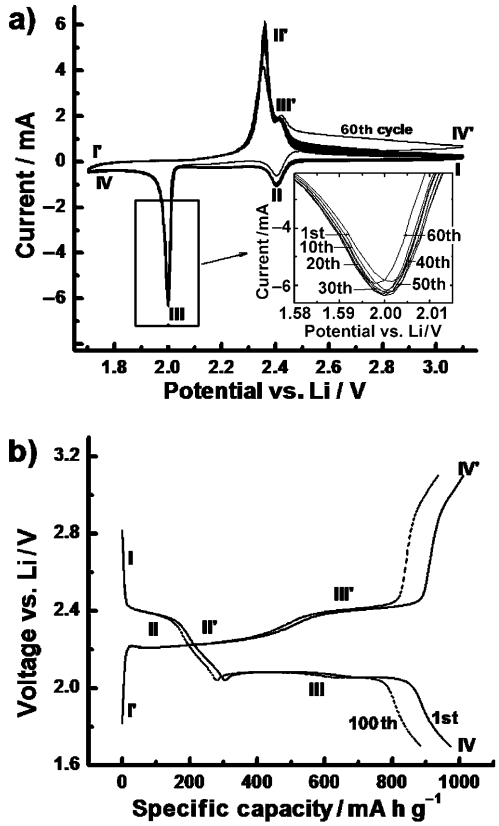

Figure 2. a) Typical cyclic voltammograms at a sweep rate 0.2 mV s^{-1} and b) voltage vs. capacity profiles under the potential window 3.1–1.7 V and at 0.5 C rate; the capacity is reported here in terms of the percentage (69.75%) of the sulfur active mass.

Figure 2a) are observed, even after 60 scans, confirming the electrochemical stability of the C@S composites and indicating that the porous carbon structure is quite effective in preventing the loss of sulfur into the electrolyte and in maintaining high utilization of the active sulfur in the redox reactions.

Figure 2b shows typical discharge/charge voltage profiles for the C@S nanocomposite. It is immediately apparent from this figure that the discharge/charge voltage plateaus, marked as II, IV, II′, and IV′, exactly resemble the redox peaks observed in the CV scans, also marked as II, IV, II′, and IV′. The oxidation peak at 2.45 V observed in our CV experiments has not been previously reported, though the corresponding charge plateau and reaction are well documented in the literature; its presence here nicely corroborates the reversibility of the electrochemical reactions occurring in the C@S nanocomposite. As shown in Figure 2b, the as-prepared C@S nanocomposites manifest an initial specific discharge capacity of 1071 mA h g^{-1} and maintains a reversible capacity of 974 mA h g^{-1} (at a rate of 0.5 C) with 91% capacity retention after 100 cycles. For completeness, Figure S8(c), reports the corresponding specific capacities in Figure 2 based on the combined mass of the C@S composite. It is evident from the figure that by either measure the specific capacity values are attractive from the point of view of applications. Additionally, no changes in the voltage plateaus are seen after 100 cycles, indicating that the electrochemical processes are substantially unchanged during extended cycling of the cell, which is also desirable for battery applications.

Figure 3 reports the voltage profile for the materials, which show the same pattern of discharge and charge plateaus even at very high current rates. The rate capability and cycle

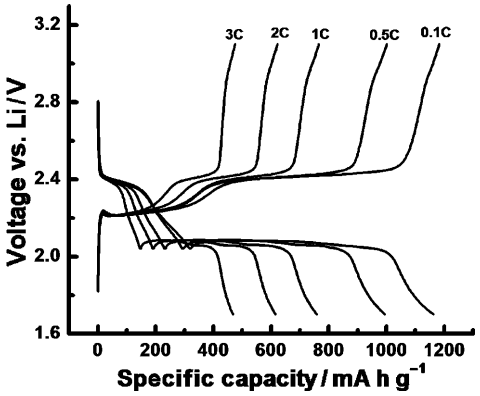

Figure 3. Typical voltage vs. capacity profiles of C@S nanocomposites at various C rates. The cell is discharged and charged at the same corresponding C rates. The capacity is reported here in terms of the percentage (69.75%) of the sulfur active mass.

life behavior of the C@S nanocomposite are considered in greater detail in Figure 4a,b. Specifically, Figure 4a shows that there is some capacity fade upon extended cycling, but reveals no evidence of the dramatic capacity reduction characteristic of Li–S cells upon extended cycling. Since the reversible Li–S_8 redox reaction occurs through the non-topotactic assimilation process, the volume expansion due to sulfur incorporated into the host carbon structure following subsequent discharge/charge reaction is anticipated to be small.[1] On the other hand, the charge/discharge behavior of pristine (unsequestered) sulfur shown in Figure S8a,b displays a notable decrease in discharge capacity and an imperfect charging characteristic for the shuttle mechanism.[4]

Once the shuttle mechanism is started, as can be seen in Figure S8(a), the charging behavior at about 2.4 V continues without overcharging, resulting in a decrease in charge efficiency at the end of the charge, and the discharge capacity is reduced.[4] The Coulombic efficiency of the C@S nanocomposite in the first cycle is computed to be 96% in comparison to 94% after 100 cycles, indicating reliable stability. In contrast, the Coulombic efficiency of pristine sulfur (Figure S8b) in the first cycle is calculated as 77%, which reduces to 31% by the end of 8 cycles. The pristine material subsequently displays the well-known continuous charging process due to an increased content of polysulfides in the electrolyte. The rate capability behavior of the C@S nanocomposite at higher rates is shown in Figure 4b. At the maximum discharge rate studied, 3C (5.1 A g^{-1}), the material is seen to deliver 450 mA h g^{-1}; an unprecedented result for a Li–S secondary battery cycled at this high rate. The stability of the cathode material is also evidenced by the recovery of a capacity of 891 mA h g^{-1} at 0.5 C rate following charging at the rather high rate (for a Li–S cell) of 3C (Figure 4b).

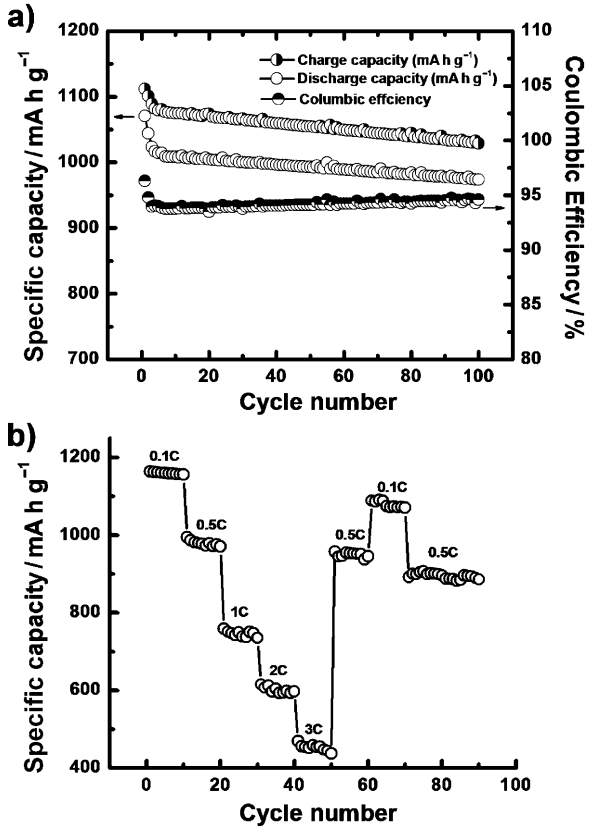

Figure 4. a) Cycle life and b) rate capability of C@S nanocomposite cells. Cycle life was carried out at a constant 0.5 C rate of discharge and charge. Rate capability study was carried out at various C rates calculated based on the percentage of sulfur active mass (69.75%) present in the C@S nanocomposite.

The excellent overall electrochemical behavior of the as-prepared C@S composites can be attributed to multiple, possibly synergistic factors that stem from their design. First, the mesoporous high surface area carbon host facilitates high levels of sulfur deposition onto, as well as into, the adsorbing carbon framework. Based on the exceptional electrochemical stability of the materials we hypothesize that confinement of sulfur in the pores and interior void space of this framework minimize loss of lithium polysulfides to the electrolyte and disfavors shuttling. Second, the partially graphitic character of the carbon framework is believed to provide mechanical stability to the deposited sulfur film and also allows good transport of electrons from/to the poorly conducting active material. We believe this latter feature is responsible for the electrochemical stability of the material at high current densities; it is expected to improve as the graphitic content of the carbon capsules increase. Finally, the pores in the framework are large enough to allow ready access by electrolyte and preserve fast transport of Li^+ ions to the active material.

In summary, a facile, scalable procedure is reported for synthesizing C@S nanocomposites based on mesoporous, hollow carbon capsules. The method uses a template-based approach for synthesizing hollow carbon particles with desirable features and vapor phase infusion of elemental sulfur into the carbon framework to produce fast, efficient uptake of elemental sulfur. When evaluated as the cathode material in a Li–S secondary battery, the as-prepared C@S nanocomposites display outstanding electrochemical features at both low and high current densities. To the best of our knowledge the materials reported herein are among the first to offer extended cycle life and high charge rate capability in a secondary Li–S battery. We attribute these observations to sequestration of elemental sulfur in the carbon capsules and to its favorable effect in limiting polysulfide shuttling, as well as to enhanced electron transport from the poorly conducting sulfur made possible by its close contact with the carbon framework.

Experimental Section

Mesoporous carbon hollow spheres were prepared by a hard template approach. In a typical synthesis, highly porous silica templates (2 g), synthesized by the method reported by Unger et al.,[21] were suspended in 50 mL of *N*-methyl-2-pyrrolidone (NMP, Aldrich) solution containing 1.05 g of petroleum pitch (Carbonix, South Korea). The suspension was sonicated for 20 min and transferred to a rotavap for distillation and complete solvent removal at 110 °C. The petroleum-pitch-coated silica particles were then vacuum dried at 110 °C for 12 h; calcination at 1300 °C for 12 h under argon flow followed. The carbon-coated silica particles obtained in this stage were treated with HF (Aldrich) to etch away the silica template and then dried after subsequent washes with water and ethanol. Sulfur incorporation was performed using the vapor phase infusion method.[19]

The C@S cathode slurry was created by mixing 92.5% of the composite (70% sulfur and 30% carbon hollow spheres) and 7.5% of PVDF binder in a NMP solvent dispersant. Positive electrodes were produced by coating the slurry on aluminum foil and drying at 120 °C for 12 h. The resulting slurry-coated aluminum foil was roll-pressed and the electrode was reduced to the required dimensions with a punching machine. The electrode thickness of the entire prepared electrodes was similar (ca. 80 μm) after 85% reduction of the original thickness through the roll press. The same procedure was followed to prepare pristine sulfur cathode, except that the cathode slurry was made of 80% of elemental sulfur, 10% of Super P conducting carbon, and 10% PVDF binder in NMP dispersant. Preliminary cell tests were conducted on 2032 coin-type cells, which were fabricated in an argon-filled glove box using lithium metal as the counter electrode and a microporous polyethylene separator. The electrolyte solution was 1M lithium bis(trifluoromethanesulfone)imide (LiTFSI) in tetraglyme.[4,5] Cyclic voltammetry studies were performed on a Solartron's Cell Test model potentiostat. Electrochemical charge–discharge analysis, under the potential window 3.1 to 1.7 V, was carried out using Maccor cycle life tester.

Received: January 25, 2011
Published online: May 17, 2011

Keywords: cathodes · electrochemistry · hollow carbon capsules · lithium–sulfur battery · shuttling

[1] X. Ji, K. T. Lee, L. F. Nazar, *Nat. Mater.* **2009**, *8*, 5000; X. Ji, L. F. Nazar, *J. Mater. Chem.* **2010**, *20*, 9821.
[2] V. S. Kolosnitsyn, E. V. Karaseva, *Russ. J. Electrochem.* **2010**, *44*, 506.

[3] J. Hassoun, B. Scrosati, *Angew. Chem.* **2010**, *122*, 2421; *Angew. Chem. Int. Ed.* **2010**, *49*, 2371; J. Hassoun, B. Scrosati, *Adv. Mater.* **2010**, *22*, 5198.
[4] C. Liang, N. J. Dudney, J. Y. Howe, *Chem. Mater.* **2009**, *21*, 4724.
[5] M. S. Song, S. C. Han, H. S. Kim, J. H. Kim, K. T. Kim, Y. M. Kang, H. J. Ahn, S. X. Dou, J. Y. Lee, *J. Electrochem. Soc.* **2004**, *151*, A791.
[6] S. R. Narayanan, S. Surampudi, A. I. Attia, C. P. Bankston, *J. Electrochem. Soc.* **1991**, *138*, 2224; M. N. Golovin, D. P. Wilkinson, J. T. Dudley, D. Holonko, S. Woo, *J. Electrochem. Soc.* **1992**, *139*, 5; T. J. Richardson, P. N. Ross, *J. Electrochem. Soc.* **1996**, *143*, 3992; M. Y. Chu, U.S. Patent 5 686 201, **1997**.
[7] Y. V. Mikhaylik, J. R. Akridge, *J. Electrochem. Soc.* **2004**, *151*, A1969; B. M. L. Rao, J. A. Shropshire, *J. Electrochem. Soc.* **1981**, *128*, 942.
[8] E. Peled, Yehuda, H. Yamin, U.S. Patent No. 4,410,609, **1983**; E. Peled, Y. Sternberg, A. Gorenshtein, Y. Lavi, *J. Electrochem. Soc.* **1989**, *136*, 1621.
[9] S. E. Cheon, K. S. Ko, J. H. Cho, S. W. Kim, E. Y. Chin, H. T. Kim, *J. Electrochem. Soc.* **2003**, *150*, A880.
[10] L. X. Yuan, J. K. Feng, X. P. Ai, Y. L. Cao, S. L. Chen, H. X. Yang, *Electrochem. Commun.* **2006**, *8*, 610; J. Wang, S. Y. Chew, Z. W. Zhao, S. Ashraf, D. Wexler, J. Chen, S. H. Ng, S. L. Chou, H. K. Liu, *Carbon* **2008**, *46*, 229; J. H. Shin, E. J. Cairns, *J. Electrochem. Soc.* **2008**, *155*, A368.
[11] J. H. Shin, E. J. Cairns, *J. Power Sources* **2008**, *177*, 537.
[12] Y. M. Lee, N. S. Choi, J. H. Park, J. K. Park, *J. Power Sources* **2003**, *119*, 964.
[13] X. M. He, Q. Shi, X. Zhou, C. R. Wan, C. Y. Jiang, *Electrochim. Acta* **2005**, *51*, 1069.
[14] S. J. Visco, M. Ying Chu, U.S. Patent, 6025094, **2000**.
[15] I. Boyano, M. Bengoechea, I. de Meatza, O. Miguel, I. Cantero, E. Ochoteco, J. Rodroleguez, M. Lira-Cant, P. G. Romero, *J. Power Sources* **2007**, *166*, 471; Y. H. Huang, J. B. Goodenough, *Chem. Mater.* **2008**, *20*, 7237; F. Wu, S. Wu, R. Chen, J. Chen, S. Chen, *Electrochem. Solid-State Lett.* **2010**, *13*, A29; J. Wang, J. Yang, J. Xie, N. Xu, *Adv. Mater.* **2002**, *14*, 963.
[16] K. Naoi, K. Kawase, M. Mori, *J. Electrochem. Soc.* **1997**, *144*, L173; N. Petr, M. Klaus, K. S. V. Santhanam, H. Otto, *Chem. Rev.* **1997**, *97*, 207; J. S. Chung, H. J. Sohn, *J. Power Sources* **2002**, *108*, 226; G. Ardel, D. Golodnitsky, K. Freedman, E. Peled, G. B. Appetecchi, P. Romagnoli, B. Scrosati, *J. Power Sources* **2002**, *110*, 152.
[17] A. Gorkovenko, US patent No. 6,210,831 B1, **2001**.
[18] J. S. Sakamoto, B. Dunn, *J. Electrochem. Soc.* **2002**, *149*, A26; S. C. Han, M. S. Song, H. Lee, H. S. Kim, H. J. Ahn, J. Y. Lee, *J. Electrochem. Soc.* **2003**, *150*, A889; B. Zhang, X. Qin, G. R. Lia, X. P. Gao, *Energy Environ. Sci.* **2010**, *3*, 153; C. Lai, X. P. Gao, B. Zhang, T. Y. Yan, Z. Zhou, *J. Phys. Chem. C* **2009**, *113*, 4712; B. Zhang, C. Lai, Z. Zhou, X. P. Gao, *Electrochim. Acta* **2009**, *54*, 3708.
[19] N. Jayaprakash, L. A. Archer, *Porous Hollow Carbon/Sulfur Composite for High Power Lithium–Sulfur Batteries*, Cornell University Invention Disclosure, ARCH-5221, **2010**.
[20] G. Katagiri, H. Ishida, A. Ishitani, *Carbon* **1988**, *26*, 565.
[21] G. Büchel, K. K. Unger, A. Matsumoto, K. Tsutsumi, *Adv. Mater.* **1998**, *10*, 1036.

